Rev. Roum. Sci. Techn.– Électrotechn. et Énerg.
Vol. **62**, *2*, pp. 165–169, Bucarest, 2017

AN INNOVATIVE HARMONIC REDUCTION STRATEGY TO ASCERTAIN THE STABILITY OF A GRID-CONNECTED PHOTOVOLTAIC SYSTEM

SOUMYA DAS[1], PRADIP KUMAR SADHU[2], BIPLAB SATPATI[3], ALOK KUMAR SHRIVASTAV[4]

Key words: Grid-connected, Photovoltaic (PV), Boost converter, PWM inverter, Transient current limiter (TCL), Stability analysis, Total harmonic distortion (THD).

Integration of significant amount of solar power, challenges the power system stability operation. Also power quality issue such as total harmonic distortion (THD) has become an increasingly serious concern as more photovoltaic cells (PV) are integrated into the grid system. This paper deals with the analysis on voltage stability and THD at the point of common coupling of a grid-connected PV system. The proposed configuration not only generates and boosts up the dc voltage, but can also convert the solar dc power into high quality ac power by means of a PWM inverter. Further, a transient current limiter (TCL) circuit has been employed here for power quality improvement as well as to ascertain the absolute stability of the overall interconnected system. Simulation and experimental results are shown for voltage and current during synchronization mode to validate the methodology for grid connection of renewable resources.

1. INTRODUCTION

Recently, with the ceasing fossil fuel and excessive rise in pollution, PV technology has emerged as one of the promising renewable energy sources due to its ability to produce electricity without any pollution. Besides this, given the strong government support, by most of the developed countries, the price of the PV system has decreased steadily over the years, especially for the grid-connected PV system. This has resulted in the rapid PV market growth in the recent years [1–3]. Electricity generated from PV power systems is one of the major renewable energy sources which involves almost zero greenhouse gas emission and doesn't consume any fossil fuel [4–6]. Generally, grid-connected renewable energy resources have location constraints since they are interconnected to the system via long transmission lines far away from load centers [7]. Proposed PV system connected with the grid is shown in Fig. 1. The work on PV generation systems, such as PV array connected through the first boost converter and three phase inverter to the grid, has eventually increased in the last decade due to the rise in demand for electric power. With the advancement and growth of power electronics, the power generated from the converters, especially the dc-dc converters and three phase inverters, can be utilized and fed to the grid. The first stage of this scheme is used to boost the PV array voltage and the second stage inverts this dc power into high quality ac power [8]. As the penetration level of photovoltaic generation increases, it will have an impact on the voltage characteristics and regulation of distribution system, and may even cause voltage instability problems, especially at those load centers [9, 10]. This paper presents the analysis on voltage stability and THD at the point of common coupling of a grid-connected PV system. This paper presents one technique, known as the harmonic current reduction control scheme for grid connected PV generation systems. This control scheme reduces harmonic current in the PV generation systems whose grid current is caused by voltage distortions at the connected grid [11, 12]. For reducing harmonic content, a transient current limiter (TCL) circuit is implemented here. It also improves the quality of the output power by minimizing the THD [13].

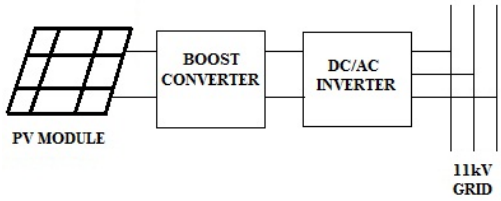

Fig. 1 – Schematic diagram of grid–connected solar PV.

2. DESCRIPTION OF THE PROPOSED MODEL

Physical model of the process under investigation is consisting of two power plants of capacity of 1000 MW and 1 200 MW respectively, synchronized at line voltage of 11 kV using step-down transformers of each having capacity 133/11 kV [14]. The schematic arrangement of the model is shown in Fig 2. In accordance with the physical model, a simulated model of the real process has been developed using Simulink to improve the power quality and ascertain the absolute stability of the overall interconnected system. Here PV array acts as a constant dc source. The detailed modelling can be found in [15, 16].

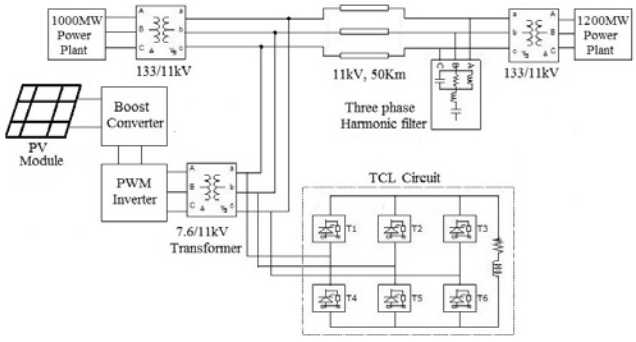

Fig. 2 – Model of proposed grid-connected solar PV system with TCL.

[1] University Institute of Technology, Department of Electrical Engineering, Burdwan, India, E-mail: soumya.sd1984@gmail.com
[2] Indian School of Mines (under MHRD, Govt. of India), Dhanbad – 826 004, India
[3] Batanagar Institute of Engineering, Management & Science, West Bengal –700 064, India

The power-conditioning unit is most frequently a dc/dc chopper. It states that the boost converter is the most suitable device for maximum power tracking. This dc/dc converter is connected between the PV array and the dc-ac converter [17]. The output of the PV array is also the input of the boost converter. Simulink model of boost converter is shown in Fig. 3.

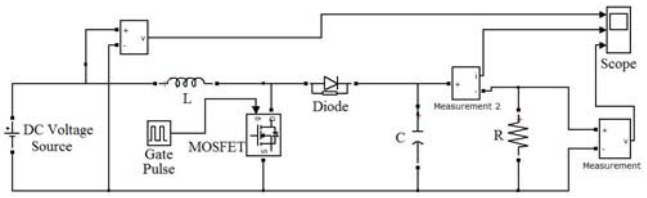

Fig. 3 – Simulink model of boost converter.

The duty ratio of chopper (α) is given by equation (1) and the chopping ratio (Y) is given by the relation (2) and (3), with t_1 as the on-time of the chopper switch (S) and T_1 as the switching period of the chopper switch (S) [18].

$$\alpha = \frac{t_1}{T_1}, \tag{1}$$

$$\frac{V_0}{V} = \frac{1}{1-\alpha}, \tag{2}$$

where v_0 is the voltage across load and V is supply voltage of converter.

$$\mathrm{Y} = \frac{\alpha}{1-\alpha}. \tag{3}$$

A 3 phase PWM inverter inverts this dc power of the chopper circuit into high quality ac power which is established here [19]. Simulink model of PWM is shown in Fig. 4. The simplest way of producing the sinusoidal pulse width modulation (SPWM) signal is by comparing a low power sine wave reference with a high frequency triangular wave. A PWM inverter yields better waveforms at no real increase in cost.

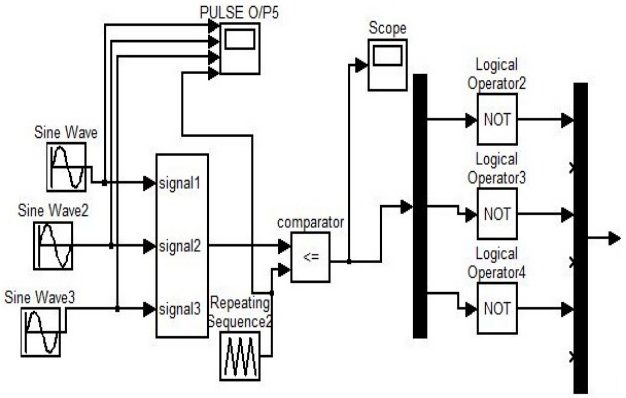

Fig. 4 – Simulink model of 3 phase PWM inverter.

The rms ac output voltage

$$V_{ac} = V_S\sqrt{\frac{p\delta}{\pi}} \rightarrow V_S\sqrt{\sum_{m=1}^{2p}\frac{\delta_m}{\pi}}, \tag{4}$$

where p = number of pulses and δ = pulse width.

Table 1

Electrical parameters of PV system power circuit

PV module	
No. of cells per module	72
Maximum power in watt	300
Open circuit voltage (V_{oc})	44.72 V
Short circuit current (I_{sc})	8.62 A
Maximum power voltage	35.86 V
Maximum power current	8.18 A
Boost chopper	
Duty cycle	0.98
Time period	10e–5
L	0.3015 H
C	4.0232e–08 F
R	48.7 kΩ
Inverter	
Power electronic device	IGBT
Number of bridge arms	3
Snubber resistance	1e5 Ω
Snubber capacitance	Infinity
TCL	
No. of thyristors	6
Resistance	0.001 Ω
Forward voltage	0.8 V
Snubber resistance	500 Ω

3. **RESULT ANALYSIS**

As discussed in the preceding section, the output voltage of the PV module is directly fed to the grid through inverter and also a step-up transformer. As penetration level of photovoltaic generation increases it may even cause voltage instability problems. That is why Transient current limiter circuit is implemented to reduce harmonics at the point of common coupling of a grid-connected photovoltaic system. The performance and stability analysis of the process under investigation are carried out using the simulated model, that is formulated, based on the physical properties of the real process. Figures 5 to 10, illustrates the impact of TCL on voltage stability of grid-connected photovoltaic system by some conventional linear stability analysis tools such as Bode, Nyquist and root locus.

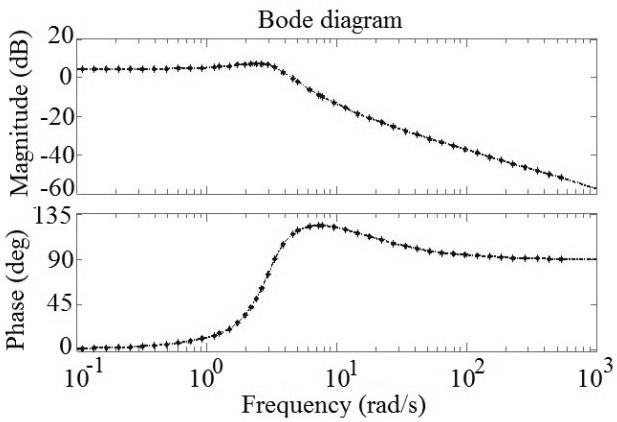

Fig. 5 – Bode plot diagram
for line voltage stability of grid without TCL.

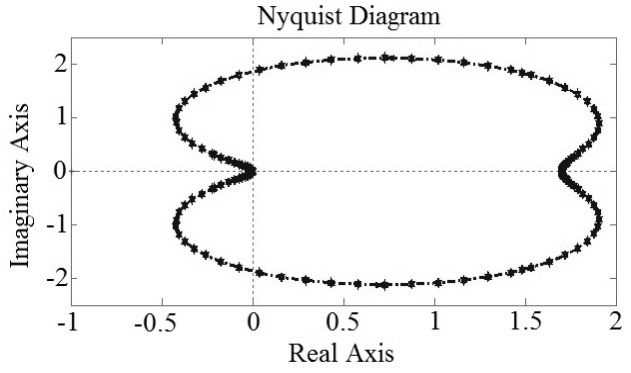

Fig. 6 – Nyquist plot diagram for line voltage stability of grid without TCL.

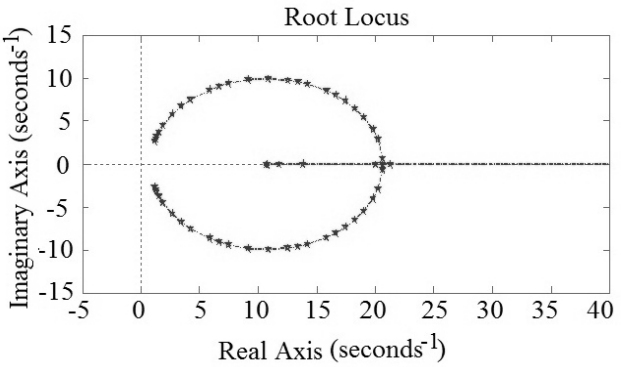

Fig. 7 – Root locus plot diagram for line voltage stability of grid without TCL.

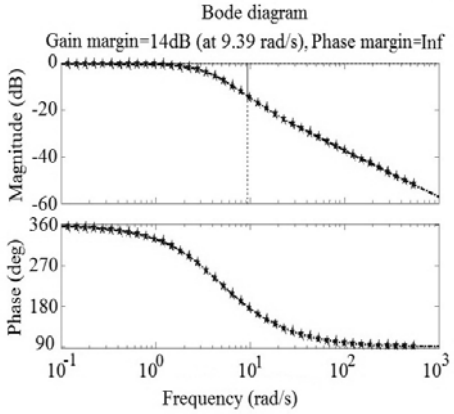

Fig. 8 – Bode plot diagram for line voltage stability of grid with TCL.

According to the stability criterion in: (i) Bode plot, a system can be stable if phase margin and gain margin are both positive, otherwise unstable; (ii) Nyquist plot, if T_{GH} contour does not encircle the critical point and the open loop system doesn't possess any open loop pole at the right half of s-plane then the system is stable; (iii) Root locus, a system may be stable if the loci corresponds to each root belongs to the open left half for a sufficiently high value of open loop gain *k*. It is evident from Figs. 5 to 7, the interconnected grid system without TCL fails to comply with the stability criteria *i.e.* gain margin: 1.2 dB and phase margin: –304.3°, which make system unstable. Further, similar type of studies was carried out for the interconnected grid system with TCL and harmonic filter and the results are presented in Figs. 8 to 10.

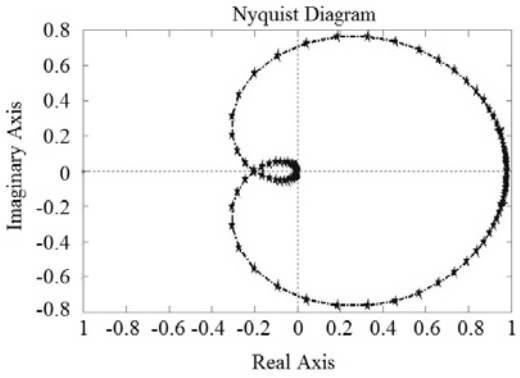

Fig. 9 – Nyquist plot diagram for line voltage stability with TCL.

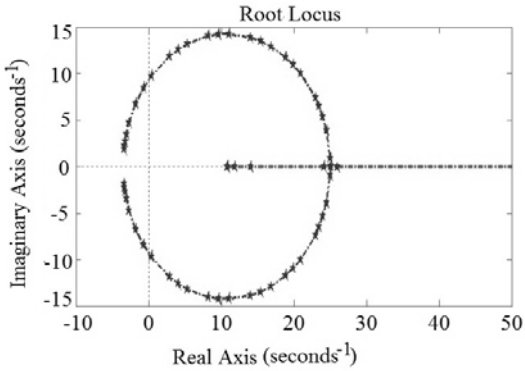

Fig. 10 – Root locus plot diagram for line voltage stability of grid with TCL.

The study reveals that the implementation of TCL with harmonic filters improves the stability of the process by a suitable amount of phase and gain margin (14 dB and infinite respectively) in comparison with interconnected grid system without TCL.

For mathematical computation of FFT analysis, let

$$N = N_1 \cdot N_2, N_1 \cdot N_2 \in N.$$

The discrete Fourier transform (DFT) of the vector $(x_0, ..., x_{N-1}) \in c^N$ is given by

$$\hat{x}_k = \sum_{j=0}^{N-1} x_j e^{-2\pi ijk/N}. \quad (5)$$

The pre-factor $\frac{1}{N}$ is omitted, since this is usually done. It can turn a one dimensional formulation of the DFT into a two dimensional one with the following change of variables

$$j = j(a,b) = aN_1 + b;\ 0 \le a \le N_2,\ 0 \le b \le N_1$$
$$k = k(c,d) = cN_2 + d;\ 0 \le c \le N_1,\ 0 \le d \le N_2.$$

It follows for $x_j = x(a,b), \hat{x}_k = \hat{x}(c,d)$ and $w_N = e^{-2\pi i/N}$,

$$\hat{x}(c,d) = \sum_{a=0}^{N_2-1} \sum_{b=0}^{N_1-1} x(a,b) w_N^{(a+N_1+b)(cN_2+d)} \quad (6)$$

$$\hat{x}(c,\tilde{d}) = \sum_{b=0}^{N_1-1} w_N^{(cN_2+d)} \underbrace{\sum_{a=0}^{N_1-1} x(a,b) w_{N_2}^{ad}}_{=:\tilde{x}(b,d)} \quad (7)$$

Since $w_N^{acN_1N_2} = w_N^{acN} = 1$ and $w_N^{adN_1} = w_{N_2}^{ad}$. This can be considered as calculating first N DFT values with length $N_2 (i.e. \tilde{x}(b,d))$ and then calculating values with length $N_2 (i.e. \tilde{x}(b,d))$ with new data $\tilde{x}(b,d)$.

FFT analysis of interconnected grid system with and without TCL is carried out simultaneously and results are presented in Figs. 11 and 12, respectively. Figure 11 shows the peak magnitude spectrum of 3-phase voltages measured in base peak with respect to the harmonic order. It is seen from the figure, that the harmonic distortions are very significant even for higher order odd harmonics. The effect of third harmonics on the corresponding fundamental phase voltages are very high. However, it is evident from Fig. 12, that the implementation of TCL circuit and harmonic filter has significantly reduced the harmonic distortion in 3-phase grid voltages. All even harmonics become almost zero and the magnitude spectrum for odd harmonics are significantly reduced to a large extent.

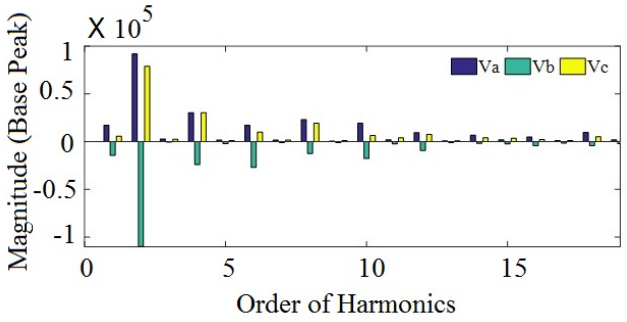

Fig. 11 – FFT analysis (Peak magnitude spectrum) of phase voltages without TCL.

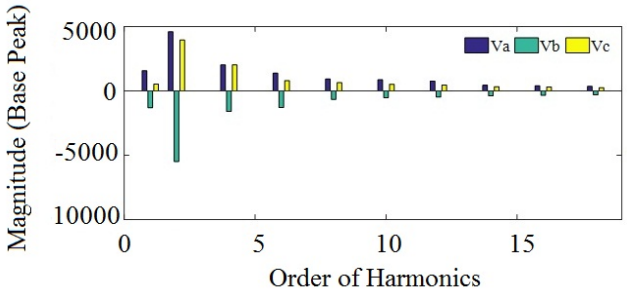

Fig. 12 – FFT analysis (Peak magnitude spectrum) of phase voltages with TCL.

Figures 13 to 16 shows the THD analysis of line voltage and phase voltage without and with TCL respectively. The expression for THD is,

$$\text{THD} = \frac{\sqrt{\sum_{n=2,3}^{\infty} V_{n\,rms}^2}}{V_{1\,rms}}. \qquad (8)$$

The percentage of voltage THD (THDv%) and its corresponding line voltage distribution is shown in Figure 13 panels (b) and (a) respectively. Figure 13b shows the value of maximum THD is 149.52 % without TCL circuit. The similar type of operation has been carried out with TCL circuit and presented in Fig. 14b and a, respectively. It is seen from the figure that, after implementation of TCL circuit at the point of common coupling of a grid-connected photovoltaic system, value of maximum THD is reduced to 54.33 %.

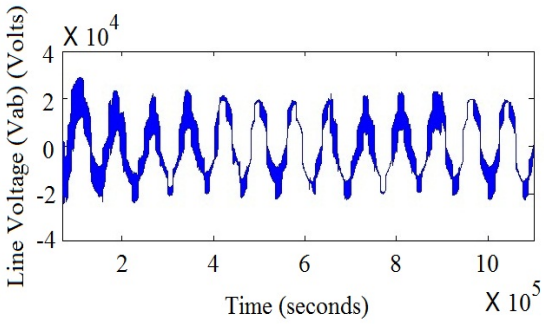

Fig. 13a – Line voltage of grid without TCL.

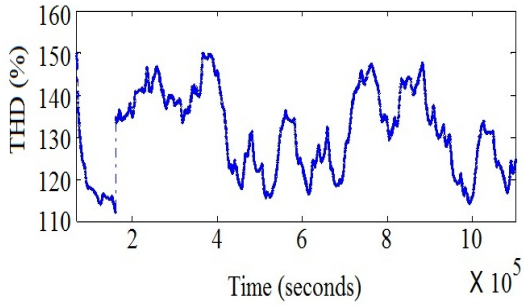

Fig. 13b – THDv(max) = 149.52 % of line voltage without TCL.

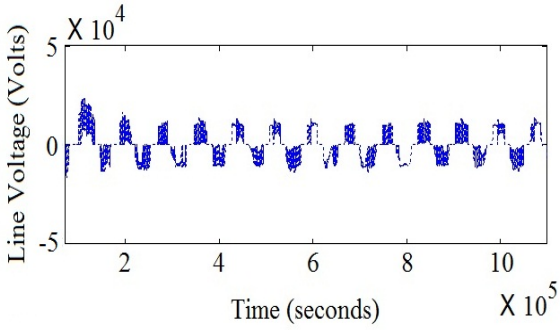

Fig. 14a – Line voltage of grid with TCL.

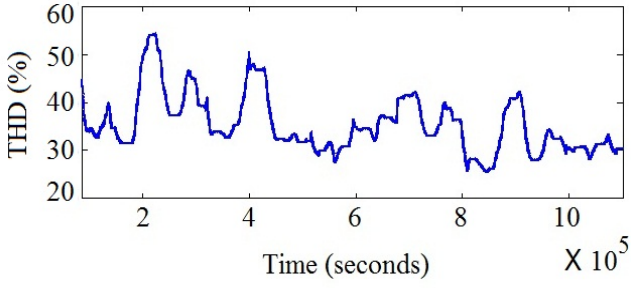

Fig. 14b – THDv(max) = 54.33% of line voltage with TCL.

The percentage of voltage THD (THDv%) and its corresponding phase voltage distribution is shown in Figure 15 panels (b) and (a) respectively. Figure 15b shows that the value of maximum THD is 375.55 % without TCL circuit. The similar type of study has been carried out with TCL circuit and presented in Fig. 16b and a respectively. It can be clearly stated from the figure that, after introducing

TCL circuit at the point of common coupling of a grid-connected photovoltaic system, maximum THD is being reduced to 54.33 %.

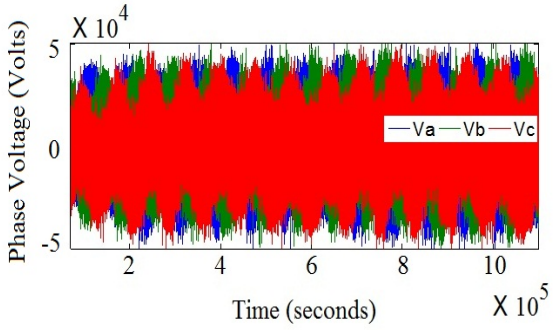

Fig. 15a – Phase voltage of grid without TCL.

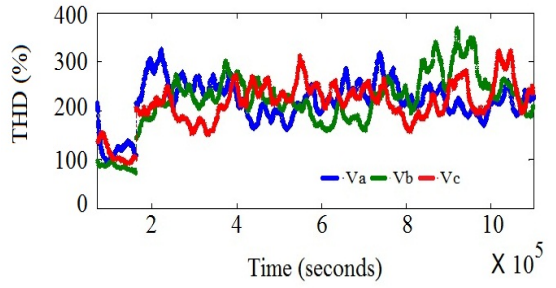

Fig. 15b – THDv(max) = 375.55% of phase voltage without TCL.

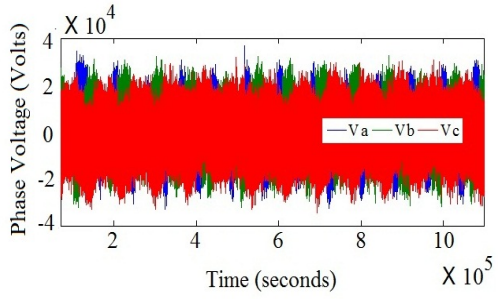

Fig. 16a – Phase voltage of grid with TCL.

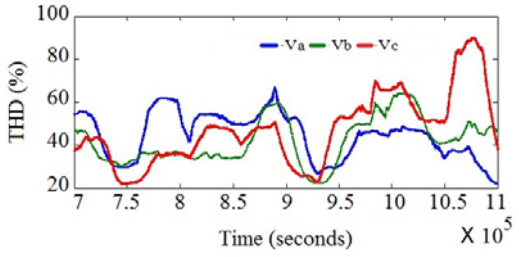

Fig. 16b – THDv(max) = 86.85 % of phase voltage with TCL.

4. CONCLUSION

This paper deals with the result of a novel analysis, based on the voltage stability and high performance harmonic reduction control scheme at the point of common coupling of a grid-connected photovoltaic system. The system has been shown to achieve the adequately accurate results with high conversion efficiency, though dc-ac conversion is required for this result. Perfect stabilization of the line voltage on the grid and power quality improvement are also successfully performed. The harmonic behaviours in terms of THDv% are also measured. The study reveals that the power quality has significantly improved by reducing the harmonic distortion and at the same time the overall stability of the interconnected system is increased to a large extent in the presence of the TCL circuit in the grid-connected PV system.

Received on January 8, 2016

REFERENCES

1. X. Cao, W. Zhang., *Grid-Connected Solar Micro Inverter Reference Design*, IEEE conference, 27–29 May 2011.
2. M. Ayub, C.K. Gan, A.F.A. Kadir, *The impact of grid-connected PV system on Harmonic Distortion*, Proc. Innovative Smart Grid Technologies-Asia, IEEE conference, 2014.
3. F. Katiraei, K. Mauch, L. Dignard-Bailey, *Integration of Photovoltaic Power System in High Penetration Cluster for Distribution Network and Mini-Grid*, International Journal of Distributed Energy Resources, **3**, *3*, 2007.
4. N. Kasa, T. Iida, H. Iwamoto, *An inverter using buck-boost type chopper circuits for popular small-scale photovoltaic power system*, IEEE, **1**, pp. 185 – 190, 1999.
5. P. Zhang, W. Li, S. Li, Y. Wang, W. Xia, *Reliability assessment of photovoltaic power systems: Review of current status and future perspectives*, Applied Energy, Science Direct, **104**, p. 822–833, 2013.
6. M. Nagao, H.Horikawa, K.Harada, *Photovoltaic system using buck-boost PWM power inverter*, Electrical Engineering in Japan, **115**, *5*, pp. 128–139, 1995.
7. Y. Zhang, C. Mensah-Bonsu, P. Walke, *Transient Over-Voltages in High Voltage Grid- Connected PV Solar Interconnection*, IEEE Conference, 2010.
8. S. Jain, V. Agarwal, *A Single-Stage Grid Connected Inverter Topology for Solar PV Systems With Maximum Power Point Tracking*, IEEE Trans. on Power Electronics, **22**, *5*, 2007.
9. Y. Xue, M. Manjrekar, Chenxi Lin, M. Tamayo, J.N. Jiang, *Voltage Stability and Sensitivity Analysis of Grid-Connected Photovoltaic Systems*, IEEE Conference, 2011.
10. W. Yang, X. Zhou, F. Xue, *Impact of large scale and high voltage level photovoltaic penetration on the security and stability of power system*, IEEE Power and Energy Engineering Conference, 2010.
11. T. Ito, H. Miyata, M. Taniguchi, T. Aihara, N. Uchiyama, H. Konishi, *Harmonic current reduction control for grid-connected PV generation systems*, IEEE International Power Electronics Conference, 2010.
12. S.A. Alexander, T. Manigandan, *Design and Development of Digital Control Strategy for Solar Photovoltaic Inverter to Improve Power Quality*, CEAI, **16**, *4*, pp. 20–29, 2014.
13. J.R. Rodriguez, F. Ruiz, D. Biel, and F. Guinjoan, *Simulation and analysis of distributed PV generation in a LV network using MATLAB-Simulink*, IEEE International Symposium on Circuits and Systems, **1**, pp. 3–6, 2010.
14. S. Das, P.K. Sadhu, A.K. Shrivastav, *Synchronization and harmonic reduction of grid connected photovoltaic system,* ICEPE international conference at NIT Meghalaya, Shillong, India, June 12–13, 2015.
15. G. Venkateswarlu, P. Sangameswar Raj, *Simscape Model of Photovoltaic Cell*, IJAREEIE, **2**, *5*, 2013.
16. S. Das, P.K. Sadhu, S. Chakraborty, N. Pal, G. Majumdar, *New Generation Solar PV Powered Sailing Boat Using Boost Chopper*, TELKOMNIKA Indonesian Journal of Electrical Engineering, **12**, *12*, pp. 8077–8084, 2014.
17. S. Bouchakour, A. Tahour, H. Sayah, K. Abdeladim, A. Abdelghani, *Direct power control of grid connected photovoltaic system with linear reoriented coordinate method as maximum power point tracking algorithm,* Rev. Roum. Sci. Techn. – Électrotechn. et Énerg., **59**, *1*, p. 57–66, 2014.
18. A.Saadi, A. Moussi, *Optimisation of Chopping ratio of Back-Boost Converter by MPPT technique with a variable reference voltage applied to the Photovoltaic Water Pumping System*, IEEE, **3**, pp. 1716–1720, 2006.
19. I. Şerban, C. Marinescu, *Power quality issues in a stand-alone microgrid based on renewable energy*, Rev. Roum. Sci. Techn. – Électrotechn. et Énerg., **53**, *3*, p. 285–293, 2008.